SOME RELATIONSHIPS OF THERMAL EFFECTS TO RUBBLE-BED STRUCTURE AND GAS-FLOW PATTERNS IN OIL SHALE RETORTS*

W. A. Sandholtz
Lawrence Livermore Laboratory,
University of California
Livermore, California 94550

ABSTRACT

To characterize bed structure and measure fluid dispersion under varied flow conditions, conventional tracer measurements in packed beds rely on detection of specific molecular species. The work reported here demonstrates the use of temperature sensors, such as thermocouples, to develop similar kinds of information from thermal data.

In oil shale retorts (that is, packed beds in which the process is driven by heat transfer from a flowing medium to the rubble), much can be inferred about bed and void structure and flow patterns from the time-temperature relationships among thermocouple arrays placed in the bed. The use of temperature data as a bed diagnostic tool in oil shale retorting experiments is shown. For combustion retorting, the close relationships between the thermal effects produced by condensing steam and those produced by retorting are illustrated. This thermal logging technique has proved useful in understanding laboratory retorting experiments and predicting retort performance.

INTRODUCTION

At Lawrence Livermore Laboratory (LLL), oil shale retort experiments (Sandholtz et. al. 1978) have shown that oil yield (measured as percent of Fischer assay) is a function of particle-size distribution in batch-combustion retorting (see table 1). In beds of broad size range, oil yield is decreased by mechanisms such as: (1) direct oil combustion where oxygen fingers into incompletely retorted regions; (2) oil cracking in high-temperature regions, either within or external to the shale particle; and (3) oil coking in slow-heating particles. Particles may heat slowly, because of either large size or localized low gas flow, resulting from low permeability regions in the bed, or both. All of these mechanisms are minimized in beds of small uniform particles. In such beds, the retorting and combustion zones tend to be well defined and small in axial dimension. Conversely, broad size ranges produce more diffuse, irregular reaction zones, neither clearly defined nor separated. This condition leads to the loss mechanisms suggested previously.

Table 1. - Oil yield in retort experiments on 80 to 100 ℓ/Mg oil shale.

Particle size range (cm)	Typical oil yield (% Fischer assay)
-2.5 + 1.3	96
-0.34 + 0.059	99
-7.6 + 0.001	88
-2.5 + 0.001	86

Because bed structure governs flow distribution in the retort and thereby determines gas dispersion, tracer tests can be useful in characterizing these packed shale beds. In batch oil-shale retorting, flow distribution is accompanied by a parallel distribution of thermal effects. That is, hot gases transferring heat to the bed will more rapidly heat regions that carry a larger proportion of the flow. They will also heat small particles (high surface-to-volume ratio) more rapidly than large particles, assuming equivalent contact with the hot gas. These are not independent effects, however, since permeability (and therefore flow) is a function of particle-size distribution and porosity. One expects bed-temperature distribution to be related, then, to these bed properties in some consistently measurable way, regardless of the flowing medium or its temperature. Examination of experimental data confirms this. Bed-temperature data can be interpreted as thermal tracers for analyzing and understanding retort-bed structure and anticipating retorting behavior (e.g., channeling and fingering of gas into the bed).

*Work performed under the auspices of the U.S. Department of Energy by the Lawrence Livermore Laboratory under contract number W-7405-ENG-48.

RESULTS

In our experimental retorts (0.3-m diam by 1.5 m and 0.9-m diam by 6.1 m), we have placed some 9 and 13 thermocouple (TC) patterns in regular planar arrays perpendicular to the retort axis. All of the TCs in a given array lie within about 1 cm of a common plane.

If a bed of small shale particles were totally uniform in size and void distribution and if such a bed were ignited uniformly and retorted (assuming a uniformly distributed gas flow), we would expect both the retorting thermal front and the combustion peak to move through the bed uniformly (see figure 1). We would expect isotherms to lie in planes perpendicular to the flow axis if the process were truly adiabatic with no radial heat loss at the retort wall.

However, if the bed structure were nonuniform in particle size or local void fraction or both, we would expect the processing zones to reflect this. We observe nonplanar isotherms, diffuse reaction zones, and increased oil loss. Using temperature data from past runs, we have been able to correlate nonuniformity of retorting and combustion zones with variations in bed structure.

We assume that slight variation of heights in the TC planar arrays produces negligible scatter in the data. We elected to compare times of arrival of the TCs in a planar array at a specified temperature. A temperature of 500°C was selected for two reasons. First, the kerogen retorting process is at or near completion at that temperature, but inorganic reactions are not yet appreciable. Second, temperature vs time data are relatively linear in this region, permitting simple interpolation of temperature data. This is shown schematically in figure 1. In the ideal case, all TCs would follow the same temperature-time trace. In the case shown in figure 1, they did not, with the result that the selected temperature (500°C) was reached at different times (t_1, t_2, t_3).

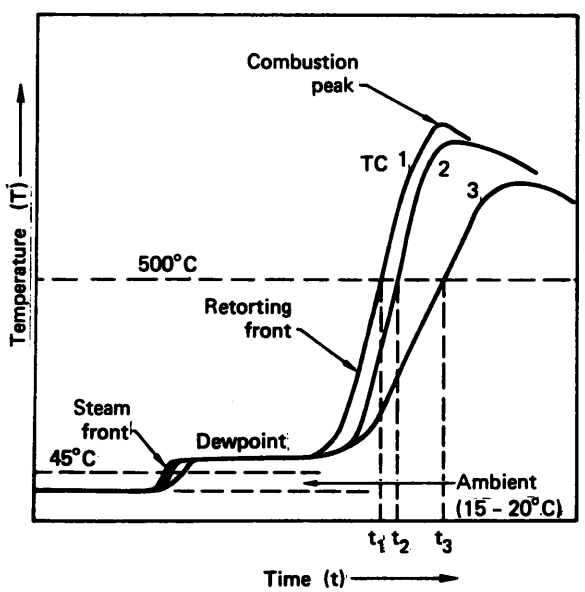

Figure 1. - Temperature as a function of time for a planar thermocouple array in a batch oil-shale retort.

This time scatter of temperature data can also be plotted as relative arrival times at a specified temperature vs position in the rubble bed (figure 2). Plotted in this way, these data give a visual concept of the general shapes of temperature isotherms, even though the ordinate is time rather than distance. For constant velocity, distance is proportional to time. Therefore, when viewed as relative distances, these plots are axially distorted to the extent that retort rates vary from point to point across the TC array. Even so, the shapes are qualitatively correct and serve to visualize flow and retorting patterns in the bed.

Real-time understanding of flow conditions during retorting could be useful in process control and in determining operating strategy. Such data, if they were available, might be even more useful as a prerun diagnostic. In discussing this possibility, Ackerman (1979) suggested the steam front that precedes the retorting front through the retort might provide just such a prerun diagnostic (see figure 1). This front is present in all combustion runs and represents the condensation of water vapor on the cool rubble. It proceeds rapidly until all the rubble is raised from ambient to dewpoint temperature. The principal sources of the water vapor are the moisture content of the shale bed, hydrocarbon combustion, and steam injected with the combustion air. Although the steam plateau temperature (dewpoint) varies with the moisture content of the retort gas, propagation of the steam front must be related to bed structure in much the same way as retorting-front propagation. In both cases, heat is being deposited in the bed from a flux of hot gas. In one case, sensible and latent heat are being deposited by the gas in the rubble bed at relatively low temperatures (less than 100°C). In the other case, primarily sensible heat deposition occurs in the same bed structure but at higher temperatures. If the bed structure is truly controlling

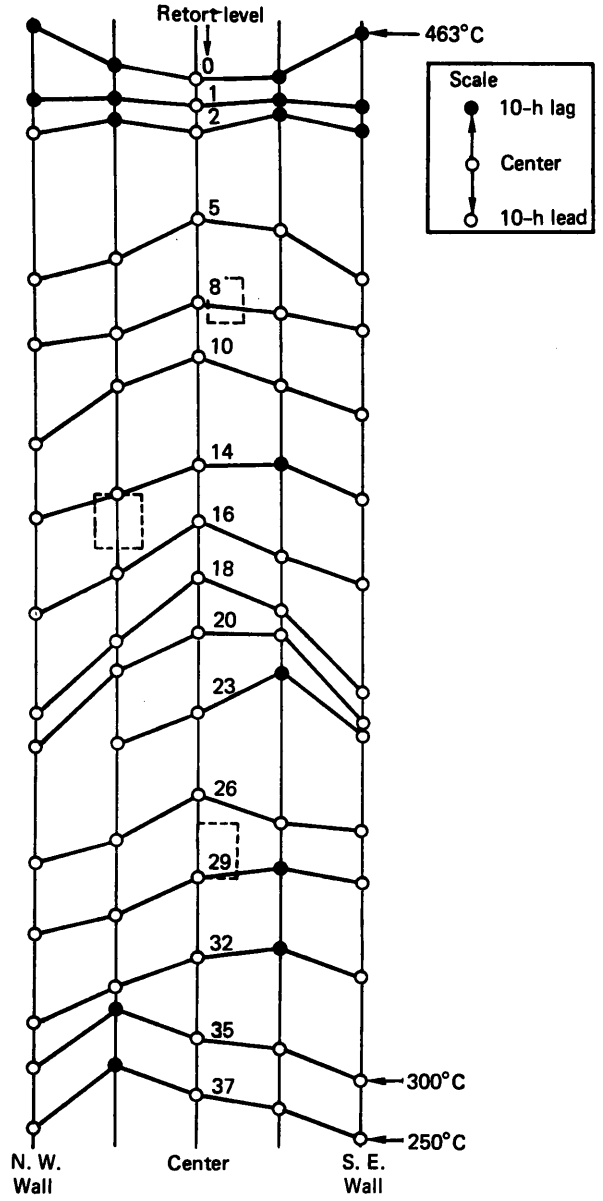

Figure 2. - Thermal profiles (Run L-3). All profiles are at 500°C unless otherwise noted.

flow, and thereby heat deposition, the two cases should correlate.

We have examined steam-front data for most of our retort experiments. Because this study was not anticipated in planning these experiments, the TC sampling rate was too slow for accurate time interpolation on the steam front. Nonetheless, the results of 10 experiments encouraged us to plan a more definitive experiment, which is described now.

In Run L-3, two grades of raw shale were charged to our 0.9-by-6.1-m retort. The lower half of the retort contained shale of about 150 ℓ/Mg (36 GPT) Fischer assay, particle sizes ranging up to about 27 cm. Overall void fraction of the bed was 0.29. The upper half of the retort bed contained shale of about 75 ℓ/Mg (18 GPT) Fischer assay, particles ranging up to 40 cm in characteristic dimension. The bed void fraction was 0.31. In this bed we installed eight planar arrays of 13 TCs each and three arrays of 9 TCs each. A schematic of this instrumentation is shown in figure 3.

The bed was ignited by a hot, inert-gas (nitrogen) preheating scheme, which brought the top portion of the bed to a high enough temperature to ignite upon the introduction of air. The remainder of the bed was combustion retorted with a steam-air mixture, which gave the 500°C isothermal profiles (previously shown in figure 2) as a function of time. In this experiment, steam-front data were taken at a sampling rate adequate for accurate interpolation and compared with the 500°C data on the retorting front. After combustion retorting was complete, the steam-front experiment was repeated three additional times on the spent shale bed at a constant steam rate but with varying noncondensable gas (nitrogen) rates. Close correlation was observed among steam-front data at all rates and on both raw and spent shale.

Good correlation was also observed between the steam-front and retorting-front data. A sample of these correlations is shown graphically in figure 4. The similarities are conspicuous. The gas- and steam-flow rates for the original retorting experiment (L-3) and the three steam-front experiments that followed (L-3A, -3B, -3C) are given in table 2. In addition

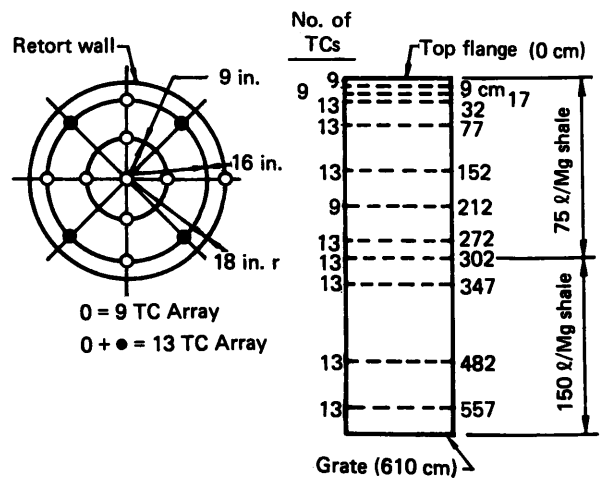

Figure 3. - Large thermocouple arrays (Run L-3).

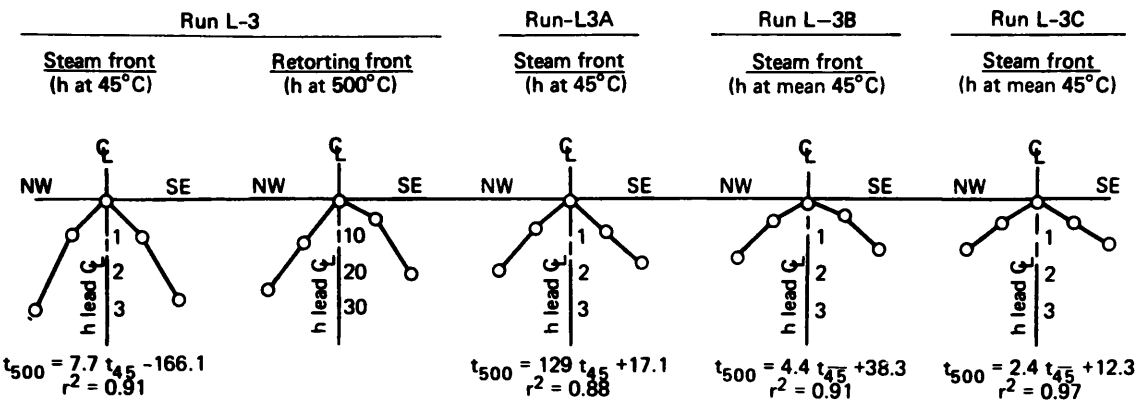

Figure 4. - Correlation of retorting-front with steam-front data (Run L-3).

to visible similarities in shapes, comparison by linear regression of the four steam fronts at 45°C with the retorting front at 500°C for each TC array, give coefficients of determination (r^2) that indicate strong correlation in most cases. Table 3 is a compilation of these results.

The coefficients of determination (r^2) in table 3 are for the general relationship

$$t_{T_1} = a + bt_{T_2} ,$$

in which the times of arrival (t) of a given TC array at specified temperatures (T_1 and T_2) are correlated. The tabulated values are for T_1 on the retorting front. As an example, the plots in figure 4 show arrival times (t) at 500°C (T_1) and 45°C (T_2) for the five TCs, across a NW to SE diameter at the 272-cm level in the rubble bed. These times for the entire 13-TC array were correlated against the times of arrival of the same TCs at 45°C on the steam front preceding the retorting front. The resulting equation is

$$t_{500} = 7.7\ t_{45} - 166.1, \quad r^2 = 0.91.$$

Similar correlations shown in figure 4 for the postrun steam experiments give the other coefficients of determination (r^2) for the chosen example (the 272-cm level).

It is tempting to conclude from the profiles in figure 2 that the prevalent concave-down shape indicates persistent channeling at the retort wall. However, this does not necessarily follow. Channeling

Table 2. - Gas rates for Run L-3 series of steam-front experiments.

Experiment	Gas	Gas/steam volume ratio	Steam rate (g/min)	Gas rate[a] (ℓ/s)	Total flow[a] (ℓ/s)	Steam front rate[b] (cm/h)
L-3	Air	1:1	180	3.7	7.4	48[c]
L-3A	Nitrogen	1:1	180	3.7	7.4	83[c]
L-3B	Nitrogen	4:1	180	15	18.7	143
L-3C	Nitrogen	1:4	180	0.9	4.6	70

[a]Standard temperature and pressure.

[b]Average rate of the mean 45°C point on the steam front.

[c]Although gas rates were the same for L-3 and L-3A, the steam front rates differ for two reasons: first, thermal properties differ greatly between raw and burned shale; and, second, L-3A started from a higher initial rubble-bed temperature.

Table 3. - Correlation of temperature data for the steam and retoring fronts (Run L-3).

Level No.	Location of TC array (cm from top flange)	Coefficients of determination (r^2)			
		Before retorting	After retorting		
		1:1 Air:steam	1:1 N_2:steam	4:1 N_2:steam	1:4 N_2:steam
0	9	[a]	0.16	[a]	0.12
1	17	[a]	0.29	0.29	0.29
2	32	[a]	0.76	0.80	0.64
5	77	[a]	0.93	0.85	0.92
10	152	0.61	0.81	0.82	0.86
14	212	0.88	0.93	0.96	0.90
18	272	0.91	0.88	0.91	0.97
20	302	0.83	0.90	0.87	0.86
23	347	0.82	0.98	0.94	0.75
32	482	0.64	0.53	0.57	[a]
37	557	0.87	0.67	0.87	0.83

[a]Data either did not exist, because of ignition procedure, or were not collected.

or cross-flow between levels will result in changed profiles.

If the data in figure 2 are replotted against lapsed time, rather than as lead- or lag-time at each level, the profiles are inverted, as in figure 5. In this plot, the results of flow nonuniformities are observable. For instance, the time lapse between Levels 2 and 5 is greater at the center line than at the wall (NW and SE); i.e., there was channeling and more rapid retorting at the wall positions. Conversely, between Levels 10 and 14, the reverse was true. The most interesting region in this plot is between levels 18 and 26; here we observe effects of gross, flow nonuniformities. Level 23 reached 500°C earlier than did Level 20 at the NW-midbed position and earlier than did Levels 18 and 20 at the centerline. Level 23 then fell behind Level 26 at the SE-midbed position. Valuable insights are gained from even these few data points. A detailed understanding of flow patterns might be realized from a greater concentration of temperature sensors in the bed volume of interest.

Consider now the steam profiles of Run L-3A that are displayed in figure 5. These are completely consistent with the 500°C profiles. We have observed previously the correlations between steam data and retorting data for a given level. Here we see the consistency from level to level.

In the data presented, we have shown the correlation between retorting data and data from thermal logging with steam. When the retorting data is quantified as level-to-level retorting rates, some understanding of flow nonuniformities can be realized. Table 4 presents ratios of rates at five positions across the NW-SE retort diameter to the rate at the retort centerline. From these data, the observations shown in table 5 are drawn.

DISCUSSION

The strong correlation shown in table 3 between the temperature data for the steam and retorting fronts indicates that the steam front can furnish valid information on bed structure and flow characteristics. Efforts to further quantify these relationships are under way. With appropriate temperature instrumentation, thermal logging with steam affords a diagnostic tool for assessing the retorting characteristics of a rubble bed before retorting. How operating and process control strategies should respond to thermal logging information must yet be determined.

The apparent lack of correlation at the top of the bed (levels 0 and 1) resulted from the ignition method used. Hot nitrogen (>500°C) was fed to the bed initially to create a bed of hot char, which was then ignited by the admission of air. This initial heating, with concomitant heat losses from

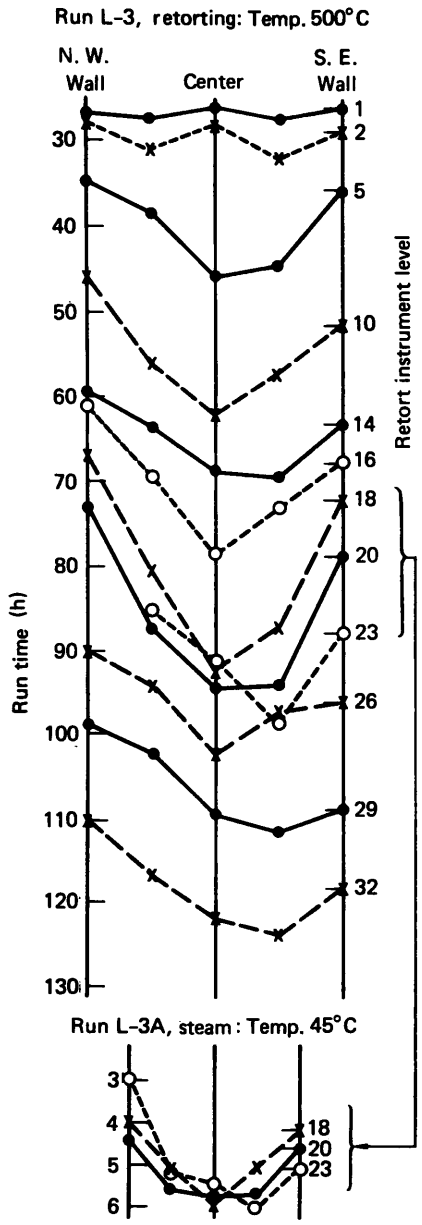

Figure 5. - Time when temperatures reached 500°C in Run L-3 and 45°C in Run L-3A.

Table 4. - Retorting rate relative to center retorting rate (Run L-3).

Retort depth range (cm)	Radial location NW	NW Mid	C	SE Mid	SE
15-30	2.3	0.6	1.0	0.5	0.8
30-75	2.7	2.3	1.0	1.5	2.8
75-150	1.6	0.9	1.0	1.4	1.0
150-210	0.5	0.9	1.0	0.6	0.6
210-240	5.1	1.9	1.0	3.0	2.3
240-270	2.6	1.4	1.0	1.0	3.4
270-300	0.4	0.3	1.0	0.3	0.4
300-345	(0.5)[a]	-1.6[b]	-1.0[b]	0.8	0.4
345-390	(0.5)[a]	1.2	1.0	-10.8[b]	1.3
390-435	1.0	1.1	1.0	0.7	0.7
435-480	1.1	0.8	1.0	1.0	1.3

[a]No 345-cm data so the rate shown is over the 300 to 390-cm range.

[b]In these zones, the lower level was retorted earlier than the upper one.

the top edges of the bed, produced heat distributions in the shale on which the initial heat of combustion was then superposed. The combined effect differed from the single thermal effect of later steam runs. The postrun steam experiments did correlate among themselves at these levels, however. We interpret this as evidence that the steam logging tests effectively and consistently responded to the bed structure, irrespective of the garbled result produced by the combined ignition and combustion effects. In other words, steam logging will yield valid bed structural information independent of the nature of earlier or later processes in the bed. This is born out in the anomalously low coefficients of determination indicated at Level 32. Here, too, both the precombustion and postcombustion steam runs correlate well among themselves. The cause of the poor correlations with the combustion run is not yet evident. At Level 10, the weaker correlation between the combustion front and the preceding steam front is an effect of the ignition process. Note that the postrun steam tests correlated well with the combustion run.

The data presented here all derive from thermocouple instrumentation, which is a convenient laboratory tool, especially when coupled with a computer system for rapid and accurate data acquisition, reduction, and tabulation. The utility of the technique in the field will depend on the ability to place and monitor appropriate temperature sensors in the rubble bed.

Actually, the lack of correlation at the Level-0 depth provides insight into the process. The Level-0 TC location was between the top of the shale bed and a layer of quartz sand used as a flow distributor. First inspection of the Level-0 data from the retort-

Table 5. - Observations of flow conditions based on rate data of table 4.

Retort depth range (cm)	Flow condition
15-30	Channeling at the NW wall.
30-75	Channeling at NW and SE walls.
75-150	Channeling persists at the NW wall, causing a downward tilt of the retorting front toward the NW.
150-210	Channeling at the center flattens the profiles, but the NW tilt persists.
210-240	Strong channeling at the wall, especially NW wall, increasing the prevailing tilt.
240-270	Wall channeling and tilt persist. The umbrella shape becomes deeper.
270-300	Center channeling dominates. The profile is flattened somewhat, but the tilt persists.
300-345	Extreme flow nonuniformity, with channeling and cross-flows, retorting Level 23 NW earlier than Level 20 NW.
345-390	Tilt is reduced.
390-435	The SE side lags, increasing tilt again. The center to NW sector is uniform.
435-480	The rate is fairly uniform across the bed diameter, with slight channeling indicated at the SE wall.

ing run intimates that the sand layer was passing the ignition gas preferentially through the center of the bed cross section. The later postrun steam-nitrogen data discounted this. It is now evident that in the ignition case heat losses at the wall, owing to poor insulation and lack of back heating in this region, dominated the situation. In the later postcombustion runs with steam, the heat loss effect was largely eliminated; and the Level-0 temperature profiles were observed to be flat, as originally expected. The good correlation observed between the steam and retorting fronts at depths below the zone preheated for ignition indicates that bed structure and not heat losses at the walls had a dominant effect on flow patterns and temperature profiles. If this were not so, heat losses at retorting temperatures would have altered temperature profiles and weakened the correlations, as was observed at the top of the bed. In Run L-3, another indication of the dominant role of bed structure was the insensitivity of the correlations between the steam and retorting fronts to large preplanned increases in heat added to the wall during the retorting phase of the experiment. We conclude that retort-wall insulation and back heating adequately served to eliminate radial heat losses as a significant factor in shaping thermal profiles.

Despite the wide variation in localized retorting rates relative to the center (shown in table 4) and the changes in thermal profiles during retorting, the overall retorting rates for each of the 13 radial positions in the retort cross section were surprisingly uniform. (Rates at a given radial position were averaged over the length of the retort.) Between Levels 5 and 32, the rates averaged 1.26 m/day with a standard deviation of only 2%. This indicates that, for this experiment, although local variations in retorting characteristics were severe, the process was nearly uniform on the 4-m height scale for which the average rates were calculated.

Table 6. - Bed and flow properties (Run L-3).

	Combustion run		Steam-logging runs		
	Steam front	Retorting front	L-3A	L-3B	L-3C
Propagation rate (m/d)	11	1.26	20	35	17
Approx. gas rate (ℓ/s)	7.4	7.4	7.4	18.7	4.6
Shale:	Raw	Raw	Burned	Burned	Burned
Specific gravity	~2.2	~2.2	~1.5	~1.5	~1.5
Porosity (%)	~0	~0	~30	~30	~30

That the correlations among the steam fronts and between the steam fronts and the retorting front are controlled by bed structure is evident when one considers the range of variables over which correlations persist. For the L-3 run series, the only invariant in the flow system was the bed geometry itself. We have observed that there is virtually no change in gross bed structure during retorting. The spent shale beds are virtually identical in internal geometry with their respective raw shale beds. Slumping and subsidence have not been observed. Where temperatures have been high enough to cause sintering, clinkering, or even melting, these have occurred after completion of kerogen retorting. Table 6 gives the range of conditions used (flow and some shale properties) for collection of the data shown in table 3. Neither the change in thermal diffusivity from raw to spent shale nor the effect of water condensation in the internal porosity of the spent shale particles in going from Run L-3A to Run L-3C is shown.

We are confident that the pattern of heat deposition in the bed is dominated by void structure (i.e., flow paths or bed geometry) and not by the heat source (sensible or latent heat) or rates of heating. The thermal properties of the bed and the porosity internal to the shale particles, over the ranges examined, do not significantly influence relative heat deposition. Therefore, steam logging correlates well, over a broad range of conditions, with the thermal behavior of the bed during retorting.

CONCLUSION

Thermal logging in which steam is used as a heat source gives valuable insight into packed-bed structure and flow distribution. In the case of beds of oil-shale rubble, steam-logging data correlate well with thermal data from subsequent combustion retorting. Thus, steam logging can be a valuable bed diagnostic tool, applicable before or during retorting, if appropriate instrumentation is installed in the bed.

ACKNOWLEDGMENTS

I am indebted to many of the members of the LLL oil-shale-project staff for helpful suggestions and technical support. I am especially indebted to Terry R. Galloway, James F. Carley, F. Jay Ackerman, and A. J. Rothman for their contributions.

REFERENCES

Ackerman, F. J., 1979, Lawrence Livermore Laboratory, personal communication.

Sandholtz, W. A., Ackerman, F. J., Rothman, A. J., Miller, W. C., Cope, E., and Ronchetto, J., 1978. The Lawrence Livermore Laboratory Oil Shale Retorts: Lawrence Livermore Laboratory, Report UCRL-52551.